



PDF hosted at the Radboud Repository of the Radboud University Nijmegen

The following full text is a publisher's version.

For additional information about this publication click this link.

<http://hdl.handle.net/2066/33012>

Please be advised that this information was generated on 2017-12-05 and may be subject to change.

Steric effects in state-to-state scattering of OH ($^2\Pi_{3/2}$, $J=3/2$, f) by HCl

R. Cireasa,^{a)} A. Moise, and J. J. ter Meulen^{b)}

*Applied Molecular Physics, Institute for Molecules and Materials, Radboud University Nijmegen,
Toernooiveld 1, 6525 ED Nijmegen, The Netherlands*

(Received 4 May 2005; accepted 1 June 2005; published online 16 August 2005)

In this paper we address stereodynamical issues in the inelastic encounters between OH ($X^2\Pi$) radicals and HCl ($X^1\Sigma^+$). The experiments were performed in a crossed molecular-beam machine at the nominal collision energy of 920 cm^{-1} . Prior to the collisions, the OH molecules were selected using a hexapole in a well-defined rotational state $v=0$, $\Omega=3/2$, $J=3/2$, $M_J=3/2$, f , and subsequently oriented in a homogeneous electrical field. We have measured rotationally resolved relative cross sections for collisions in which OH is oriented with either the O side or the H side towards HCl, from which we have calculated the corresponding steric asymmetry factors S . The results are presented in comparison with data previously obtained by our group for the inelastic scattering of OH by CO ($E_{\text{coll}}=985 \text{ cm}^{-1}$) and N_2 ($E_{\text{coll}}=985 \text{ cm}^{-1}$) studied under similar experimental conditions. The dissimilarity in the behavior of the OH+HCl system revealed by this comparison is explained on the basis of the difference in the anisotropy of the interaction potential governing the collisions. The interpretation of the data takes into account the specific features of both nonreactive and reactive parts of the potential-energy surface. The results indicate that the scattering dynamics at this collision energy may be influenced by the HO–HCl van der Waals well and by reorientation effects determined by the long-range electrostatic forces and, furthermore, may involve reactive collisions. © 2005 American Institute of Physics. [DOI: 10.1063/1.1978874]

I. INTRODUCTION

The dependence of the dynamics on the orientation of the colliding partners represents a key issue for molecular collision processes. In particular, the reactivity of the system depends not only on the reaction barrier height, but also on the relative orientation of the reactants before and during reactions.¹ Consequently, the development of techniques for molecular axis alignment or orientation has become an important goal in the field of reaction dynamics. The techniques available to date employ collisional processes, optical, and/or static electrical fields in order to achieve the desired alignment/orientation. The first method is based on the collision processes present in the supersonic expansions used to produce molecular beams.^{2–4} The collisions between the molecules induce a preferential alignment of their rotational angular momentum perpendicular to the flight axis, thus creating an anisotropic spatial distribution of the molecular axes. An alternative approach is based on the use of polarized laser radiation to align molecules.^{5–7} An optical laser field resonant with a parallel or perpendicular transition of the molecule imposes an alignment of the randomly distributed rotational angular momentum. With this method it is possible to create samples of aligned molecules in the ground or excited vibrational/electronic states. The main drawback of this technique is related to the fact that only a small per-

centage of the molecules will be aligned, depending on the absorption cross section for the selected transition and the laser intensity employed. The advent of powerful lasers has made it possible to produce much stronger alignment using polarized femtosecond laser radiation.⁸ In turn, the use of the static electrical fields allows not only the alignment, but also the orientation of molecules. Actually, there are two methods to control the orientation by electrical fields: brute force orientation^{9–11} and hexapole state selection and orientation.^{12–14} While the first one employs very strong homogeneous fields to orient polar molecules, the other uses weak homogeneous fields preceded by hexapole fields. The radial field of the hexapole focuses only the trajectories of molecules in a particular quantum state, creating the so-called molecular state selection and a local orientation. A subsequent weak homogeneous field is necessary in order to achieve the desired orientation. The need for improvement and generalization of the orientation techniques led recently to a new method combining strong optical fields with static electrical fields.^{15,16}

The orientation issues also received a lot of interest from a theoretical point of view, primarily in connection with the field of dynamical stereochemistry. For theoreticians, the term “orientation” has a different definition and it is expressed in the molecular frame, while the experimental orientation is expressed in the laboratory frame. Whereas in the experimental case, the concept of orientation refers to the relative orientation of reagents before the collision process, the theoretical models consider their relative orientation at the reaction barrier. Therefore, it is intimately related to the so-called cone of acceptance, defined in terms of steric re-

^{a)}Current address: Physical and Theoretical Chemistry Laboratory, University of Oxford, South Parks Road, Oxford OX1 3QZ, United Kingdom; permanent address: Laser Department, National Institute for Laser, Plasma and Radiation Physics, P.O. Box MG-36, Bucharest, Romania.

^{b)}Author to whom correspondence should be addressed. Electronic mail: H.terMeulen@science.ru.nl

quirements imposed by the orientation dependence of the reaction barrier height.^{1,17} The idea of cone of acceptance through which the collision trajectories must pass in order to access the transition state (TS) and to become reactive is derived from the angle-dependent line of center (ADLOC) model.^{18–20} In this model the barrier is chosen to depend on the angle of attack defined between the symmetry axis of the molecule and the line connecting the centers of mass of the reactants. Generally, the correspondence between the experimental and theoretical orientations is not unique.²¹

Most of the experimental and theoretical works on orientational effects are devoted to the study of the reactive scattering processes (see reviews from Refs. 22 and 23). The first measurements of steric effects in inelastic collisions were reported by Stolte and co-workers. They have performed state-to-state investigations of collisions between NO and Ar or He, in which NO was state selected and oriented by means of static electrical fields.^{24–27} Both systems exhibit quite a peculiar aspect in the sense that the steric asymmetry factors had an oscillatory behavior also reproduced by quantum scattering calculations. Using the same technique, our group tackled the stereodynamics of the inelastic collisions between OH and several atomic and molecular collision partners. Like NO, OH is an open-shell molecule, but its rotational structure is described by the intermediate Hund's case coupling and thus behaves differently from NO in inelastic collisions. Steric asymmetry measurements were first reported for the scattering of OH by He, Ar, *n*-H₂, and *p*-H₂.²⁸ Subsequently, results of orientational effects for OH–CO and OH–N₂ systems were obtained with improved detection sensitivity.²⁹ The availability of high quality *ab initio* potential-energy surfaces (PESs) enabled a joint experimental and theoretical study of the OH–Ar system.³⁰ The agreement of the experimental steric factors with those obtained by quantum scattering calculations illustrates the great potential of inelastic-scattering experiments in assessing the accuracy of the PESs employed.

In this paper we address the stereodynamical issues of the inelastic scattering between OH and HCl. The study was carried out in a crossed molecular-beam setup at the collision energy of 920 cm^{−1}. By means of static electrical fields, the OH reagent was selected in a single-quantum state, $v=0$, $\Omega=3/2$, $J=3/2$, $M_J=3/2$, f , and was oriented with either the O side or the H side pointing towards HCl. We have defined a steric asymmetry factor S as the ratio between the difference and the sum of the relative cross sections for each orientation. S is measured as a function of the Λ -doublet symmetry of the OH final rotational state for the scattering into either spin-orbit manifolds. The values of S are discussed in comparison with those obtained for collisions of OH with CO and N₂ at a similar collision energy ($E_{\text{coll}}=985$ cm^{−1}) and under similar experimental conditions. For the interpretation of the magnitude and the sign of the steric asymmetry factor, the dynamical relevant features of both nonreactive and reactive parts of the PESs are considered.

II. EXPERIMENTAL SETUP

The experimental setup presented in Fig. 1 is identical to that used previously for state-to-state inelastic scattering ex-

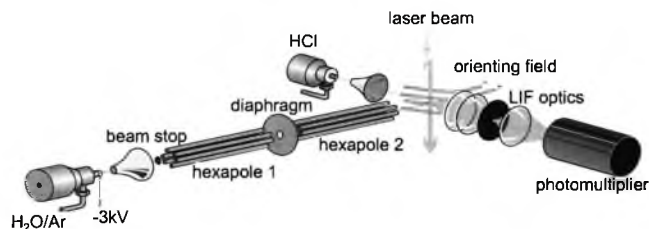


FIG. 1. Schematic representation of the experimental setup.

periments between oriented OH and Ar.³⁰ Four parallel stainless steel rods have been inserted into the collision region for the orientation of the OH radicals. Both molecular beams with typical pulse widths of 40–50 μ s were obtained by expanding the gas mixtures through pulsed-current loop valves (Jordan Inc.). The HCl ($X^1\Sigma^+$) beam was produced by expanding pure HCl through a 0.5-mm-diameter nozzle. In order to ensure the single-collision regime, the backing pressure was chosen to be around 530 ± 30 Torr. From resonantly enhanced multiphoton ionization (REMPI) ($1+1'$) measurements of the $V^1\Sigma^+-X^1\Sigma^+$ transition around 118 nm, the rotational temperature was determined to be 20 ± 5 K. At a distance of 85 mm from the nozzle exit, the HCl beam was crossed at right angle by the OH ($X^2\Pi$) beam. The OH beam was created by means of a pulsed discharge established at the nozzle exit in a mixture of 4% H₂O vapor and Ar at the pressure of 600 Torr. The collision energy was estimated to be 920 cm^{−1} with a spread [full width at half maximum (FWHM)] of 250 cm^{−1}.

The initial rotational distribution of the OH beam ($T_{\text{rot}} \approx 35$ K) obtained by supersonic cooling was reduced to a single-quantum state distribution ($\Omega=3/2$, $J=3/2$, $M_J=3/2$, f) by using the spatial focusing properties of the hexapoles. A positive voltage of 23 kV was applied to every other rod of the hexapoles, while the other rods were kept at ground potential, in order to focus only the OH radicals in the desired state in the collision region located 36 cm away from the nozzle exit. The rotational distribution of the molecular beam in the collision region consisted of 93.3% OH in the $\Omega=3/2$, $J=3/2$, f state and about 4% in the $\Omega=3/2$, $J=5/2$, f state, with the rest of the molecules being distributed among 11 other rotational states. The ratio of the M_J state populations, $|M_{J=3/2}|/|M_{J=1/2}|$, in the $J=3/2$ state was measured to be 15.8. An extensive description of the electrostatic state selection method and of the technical characteristics of the hexapoles is given in Refs. 28 and 30.

Prior to the collisions with HCl molecules, the OH radicals are oriented in a static electrical field created by a ± 12 kV voltage applied pairwise on the four rods. The direction of the electrical field was set parallel to the relative velocity and its orientation was changed by switching the polarity of the rods. The OH radicals could therefore be oriented with either the O side or the H side towards the HCl partner. The degree of the orientation can be quantified using the following formula:

$$\langle \cos \theta \rangle_{M_J}(E) = 2\alpha_{M_J}(E)\beta_{M_J}(E) \frac{\Omega M_J}{J(J+1)}, \quad (1)$$

where θ is the angle between the molecular axis and the electrical field axis and J , Ω , and M_J are the total angular

momentum and its projections onto the molecular and electrical field axis, respectively. $\alpha_{M_J}(E)$ and $\beta_{M_J}(E)$ represent the coefficients used to express the total electronic wave function in the electrical field, $|JM_J\Omega E\rangle$, as a linear combination of the field-free wave functions $|JM_J\Omega e\rangle$ and $|JM_J\Omega f\rangle$:

$$|JM_J\Omega E\rangle = \alpha_{M_J}(E)|JM_J\Omega e\rangle + \beta_{M_J}(E)|JM_J\Omega f\rangle. \quad (2)$$

At the value of the electrical field used in this experiment, 7.5 kV/cm, the degree of mixing between states of e and f symmetries is rather small, thus these states could generally be labeled using this convention.^{30,31} For the present conditions, the degree of orientation was determined to be $\langle \cos \theta \rangle = 0.549$ close to the maximum theoretical value of 0.6, obtainable in the high electric-field limit for molecules in the $\Omega=3/2$, $J=3/2$, $M_J=3/2$ state. The electrical field homogeneity across the collision region was checked as described in Ref. 30 in order to make sure that all the molecules were subjected to the same orientating force. More details on the orientation of molecules in static electrical fields and on the determination of the degree of the orientation can be found in Refs. 28 and 30.

The rotational distribution of the scattered OH radicals, as well as their initial state distribution was probed by the saturated laser-induced fluorescence (LIF) method. A Nd:yttrium aluminum garnet (YAG) pumped dye laser (Continuum TDL-60+Continuum 681C) operating at 10 Hz was used to produce by frequency doubling the radiation at around 308 nm necessary for the excitation of the $A^2\Sigma^+(v'=0)-X^2\Pi(v=0)$ transition. The laser beam was polarized using a beam splitter cube polarizer and a $\lambda/2$ plate in order to get the best signal-to-noise ratio for the fluorescence. The polarization axis was set at an angle different from 0° or 90° with respect to the electrical field axis in order to allow the unbiased detection of the population of all M_J substates. Power-broadening effects were avoided by using typical laser energies of about 0.5–0.8 mJ/pulse. A probe beam with a homogeneous intensity distribution was obtained by cutting off the low-energy wings of the laser beam spatial profile. The transitions of the P_1 or Q_2 branches were used to probe e state populations, whereas the f state populations were measured via $Q_1(J)$ or $P_2(J)$ transitions. Note that the $Q_2(2)$ and $Q_2(3)$ lines cannot be resolved within the laser bandwidth of 0.45 cm^{-1} , therefore the $\Omega=1/2$, $J=3/2$, e and $\Omega=1/2$, $J=5/2$, e state populations were probed simultaneously. All measurements were performed with the laser wavelength parked at the transition peaks. The OH fluorescence was optically and spatially filtered and imaged onto the photomultiplier tube EMI 9235QB. The output of the photomultiplier was amplified five times and subsequently gated and integrated using a boxcar averager. The discrimination between the collision-induced population and the initial state population was made by altering the delay of the HCl beam with respect to the collision event from 0 to 10 ms. State-resolved cross sections were measured for collisions in which OH was oriented with either the O side or the H side towards HCl. An averaging over 2000 laser shots was performed for each orientation. In order to compensate for experimental drifts in laser

energy and alignment, the measurement session was composed of three consecutive sequences: one of 1000 laser shots for one of the two OH orientations followed by a block of 2000 laser shots for the opposite orientation and again by a sequence of 1000 laser shots for the initial OH orientation.

III. DATA ANALYSIS

In order to quantify the influence of the relative orientation of the OH radical in the scattering process, we define a steric asymmetry factor as follows:

$$S = \frac{\sigma_{\text{HO-HCl}} - \sigma_{\text{OH-HCl}}}{\sigma_{\text{HO-HCl}} + \sigma_{\text{OH-HCl}}} \times 100 \% . \quad (3)$$

The $\sigma_{\text{HO-HCl}}$ and $\sigma_{\text{OH-HCl}}$ cross sections represent the relative state-to-state cross sections for the collisions in which OH is oriented towards HCl with the O side and the H side, respectively. A positive value of S would indicate that the cross section for the collision at the O side is the largest, while a negative value would correspond to the opposite situation.

As shown previously,³¹ the relative state-to-state collision cross section, $\sigma_{i \rightarrow f}$, for scattering out of the initial state i into a final state f can be calculated using the following formula:

$$\sigma_{i \rightarrow f} \propto \frac{\delta S_{ff'}}{n_i L_{ff'} P_{ff'} F_f}, \quad (4)$$

in which $\delta S_{ff'}$ represents the scattering signal obtained by subtraction of the fluorescence signal corresponding to the initial population from the fluorescence signal corresponding to the final population of the state f , n_i represents the population density of the initial state before collisions, $L_{ff'}$ represents the rotational line strength of the transition used to probe the f state, $P_{ff'}$ is the laser power at the excitation frequency, and F is the flux-to-density transformation factor. Consequently, in the saturation limit, the “state-to-state” steric asymmetry factor can be determined directly from the scattering signal $\delta S_{ff'}$ as the other factors cancel out. The detection sensitivity is similar, regardless of the final state of the scattered molecules, due to the small spread in the kinetic-energy release³² and consequently, a comparable “residence time” in the detection region of all scattered molecules. In these conditions, we have defined a detection region which exceeded the dimension of the collision region in order to ensure the detection of all the scattered molecules. For each quantum state, S was averaged over six to 45 measurements. The error bars were calculated using a weighted statistical analysis.

IV. RESULTS AND DISCUSSION

Before presenting the results, it should be recalled that the experiments of inelastic scattering performed without orienting the OH radicals pointed to an inefficient rotational energy transfer (RET): only approximately 40% of the kinetic energy was transferred into internal energy. Generally, a propensity was found for spin-orbit-conserving transitions, but no propensity for excitation into a particular Λ -doublet component of the same rotational state was evident.³²

TABLE I. Steric asymmetry factors measured for inelastic collisions of OH with HCl presented in comparison with the steric asymmetry factors obtained for the scattering of OH by CO and N₂ (Ref. 29). The errors represent one standard deviation and for OH+HCl were obtained using a weighted statistical analysis.

Final state			OH+HCl	OH+CO	OH+N ₂
Ω	J'	ϵ	$E_{\text{coll}}=920 \text{ cm}^{-1}$	$E_{\text{coll}}=985 \text{ cm}^{-1}$	$E_{\text{coll}}=985 \text{ cm}^{-1}$
3/2	5/2	<i>e</i>	3.0 ± 1.2	-1.6 ± 0.5	1.1 ± 0.7
	5/2	<i>f</i>	-16.5 ± 1.6	23.2 ± 1.6	25.2 ± 1.9
	7/2	<i>e</i>	-1.1 ± 3.5	-8.8 ± 0.8	-4.9 ± 1.1
	7/2	<i>f</i>	-21.3 ± 5.4	-23.4 ± 2.8	-17.7 ± 3.1
	9/2	<i>e</i>	18.8 ± 12.4	-17.7 ± 3.5	-5.5 ± 2.6
	9/2	<i>f</i>	-5.28 ± 6.53	-29.4 ± 7.2	-7.0 ± 3.9
1/2	1/2	<i>e</i>	6.7 ± 4.0	-3.3 ± 0.7	-13.4 ± 1.0
	1/2	<i>f</i>	-0.3 ± 3.7	10.2 ± 1.0	1.1 ± 1.8
	3/2 and 5/2	<i>e</i> ^a	7.1 ± 3.3	-6.4 ± 0.8	-5.3 ± 1.2
	3/2	<i>f</i>	9.2 ± 8.6	11.8 ± 1.3	4.3 ± 1.9
	5/2	<i>f</i>	-22.2 ± 10.6	-6.6 ± 1.8	-4.9 ± 2.1

^aThe measured steric asymmetry factor contains contributions from both 3/2*e* and 5/2*e* states as the absorption lines used to probe them could not be resolved within the laser bandwidth.

The values of the steric asymmetry factors measured for collisions of OH with HCl are displayed in Table I and Fig. 2. Due to the absence of other experimental or theoretical data, the discussion of these results will be presented in comparison with those previously obtained by our group for the inelastic collisions of oriented OH with CO and N₂.²⁹ For convenience, the steric factors measured for these two systems are displayed in Table I and Fig. 3. As can be seen from Table I, the steric factor measured for OH+HCl system depends on the spin-orbit manifold and on the Λ -doublet symmetry of the final state and varies between 18.8% for the $\Omega=3/2$, $J=9/2$, *e* state and -21.3% for the $\Omega=3/2$, $J=7/2$, *f* state for spin-orbit-conserving transitions, and between 9.2% for the $\Omega=1/2$, $J=7/2$, *f* state and -22.2% for the $\Omega=1/2$, $J=5/2$ state for spin-orbit changing collisions. The overall variation is similar to that observed for the OH+N₂ system, for which S varied from 25.2% for the $\Omega=3/2$, $J=5/2$, *f* state to -17.7% for the $\Omega=3/2$, $J=7/2$, *f* state, but slightly lower than that measured for the OH

+CO system, for which S varied between 23.2% for the $\Omega=3/2$, $J=5/2$, *f* state to -29.4% for the $\Omega=3/2$, $J=9/2$, *f* state. It is interesting to note that for all the collision partners the highest absolute values of the steric asymmetry factors were generally found for spin-orbit-conserving transitions. For scattering into rotational states of the same spin-orbit manifold, $\Omega=3/2$, we measured negative values for symmetry-conserving transitions and zero or positive values for symmetry-changing transitions. In turn, for spin-orbit-changing transitions $\Omega=3/2 \rightarrow \Omega=1/2$, S is slightly positive and almost independent of the final rotational state and its Λ -doublet symmetry, except for the negative value measured for the excitation into the $\Omega=1/2$, $J=5/2$, *f* state. This behavior is different from that measured for collisions between OH and CO or N₂. Generally, for these systems, S exhibits a quasimonotonical dependence with the rotational quantum number of the final state, with positive values at low J and negative ones at high J . An intuitive reasoning can be used to describe such generic behavior. Considering that the un-

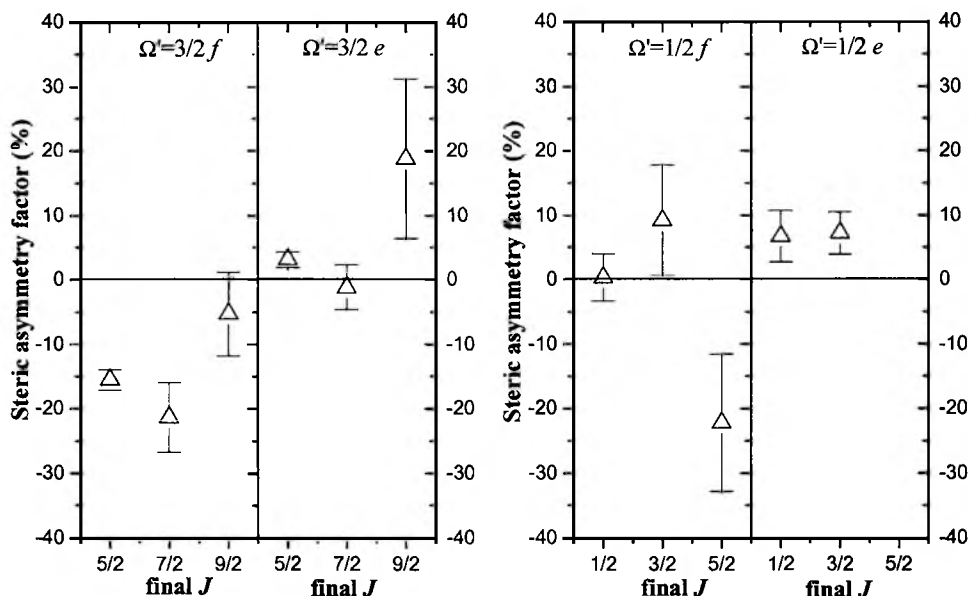


FIG. 2. Steric asymmetry factor for inelastic collisions of OH with HCl, measured at the collision energy of 920 cm⁻¹. The final spin-orbit state and the Λ -doublet symmetry are indicated at the top each panel.

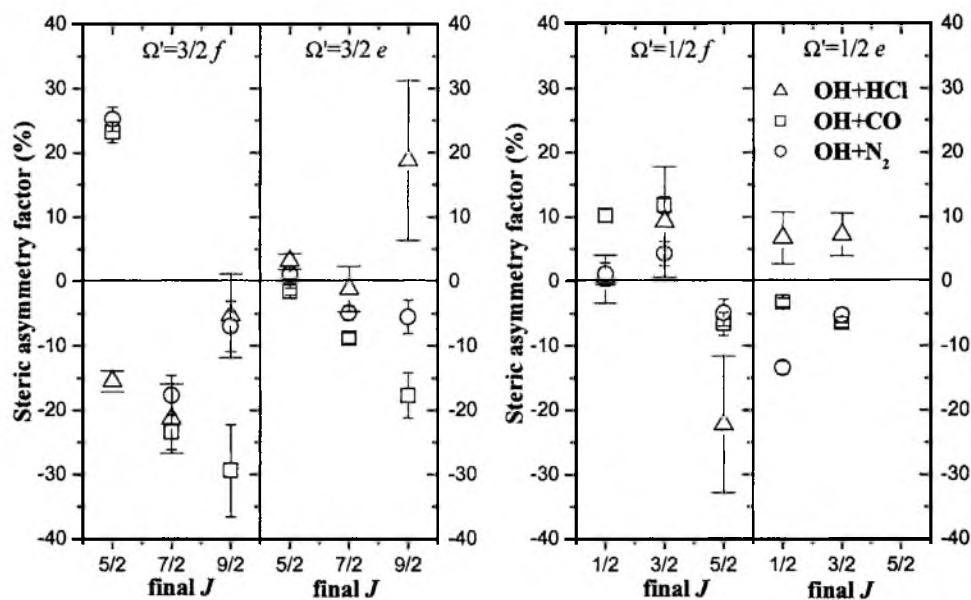


FIG. 3. Steric asymmetry factor for inelastic collisions of OH with HCl, CO, and N₂ measured at the collision energies of 920, 985, and 985 cm⁻¹, respectively. The final spin-orbit state and the Λ -doublet symmetry are indicated at the top of each panel.

paired electron occupying the π orbital is located closer to the O atom, one might expect a propensity for collisions at the O side (positive S). Conversely, the preference for collisions at the H side (negative S) observed for excitation into high rotational states could be pictured in a classical manner using the ball-and-stick model. It is more efficient to exert a large torque, needed for high rotational excitations, at the H side as it is farther away from the center of mass. These models were used to rationalize the rotational dependence of S observed in the collisions of OH with the “spherical” Ar atom.³⁰ Nevertheless, these simplistic explanations cannot be used to describe the behavior of the OH+HCl system for which the intermolecular interactions are much stronger due to the existence of quadrupole and dipole moments.

While for collisions with CO and N₂ the steric asymmetry factor is positive for the excitation into the lowest rotational state, $\Omega=3/2$, $J=5/2$, f , the collisions between OH and HCl lead to a negative S with an absolute value of 16.5 ± 1.6 . This result represents the most striking difference in the behavior of the OH+HCl system as compared with the OH+CO and OH+N₂ systems. Basically, a negative value for S means that a smaller number of OH molecules was detected in the final state after collisions at the O side than upon collisions at the H side. This corresponds to larger inelastic cross sections for the scattering at the H side, but could also be an indication that a part of the OH molecules colliding with the O side are “removed” from the detection region. We should recall here that for each quantum state, the collision signals for both orientations were recorded in the same measurement session. In particular, for scattering into the lowest rotational state, $\Omega=3/2$, $J=5/2$, f , the steric factor was obtained by averaging over a set of 45 measurements recorded over a widespread period of time, indicating that its negative sign is not due to an experimental artifact.

The negative value for S is due to the anisotropy of the interaction potential with respect to the approach of HCl molecules to one or the other end of the OH radical. Therefore, by examining the landscape of the PES we can obtain information to explain this behavior. The existence of strong

dipole moments for both HCl and OH determines strong long-range electrostatic interactions which lead to the formation of van der Waals wells. It was found using different levels of theory^{33–37} that the deepest van der Waals well is located at the O side of the OH radical and its depth was estimated in the range 870–1900 cm⁻¹. *Ab initio* calculations employing quadratic configuration interaction with single, double, and perturbative triple excitation (QCISD(T))³⁴ found on the ground-state $^2A''$ potential surface a planar L-shaped HO–HCl complex ($\theta_{\text{HOH}}=112^\circ$ and $\theta_{\text{OHC}}=174^\circ$), with a binding energy of 1100 and 550 cm⁻¹ when the zero-point energy is included. Similar complex geometry and dissociation energy were obtained from restricted coupled cluster with single, double, and perturbative triple excitation calculations (RCCSD(T)) on the lowest adiabatic surface $^2A''$ and on the diabatic surface V_{sum} , expressed as the average of the two adiabats $^2A''$ and $^2A'$.^{35,36} Three other weaker complexes were found using the QCISD(T) method, but only one resulted in an intermolecular bond at the H side ($D_0 \approx 250$ cm⁻¹) located on the excited potential surface, $^2A'$. Exploring the PES landscape farther into the reactive region, an early transition state (TS) can be located in the entrance channel of the $^2A'$ surface. The geometry of the TS is bent and nonplanar with a H–O–H angle (103°) similar to the angle formed by the bonds of the H₂O product.^{33,34,37,38} In turn, the geometry is quasilinear with respect to the approach of the HCl molecule ($\theta_{\text{OHC}}=143^\circ$ – 156°), as typically found for the heavy-light-heavy reaction type. The TS correlates to the HO–HCl complex via a conical intersection between the $^2A'$ and $^2A''$ surfaces. Moreover, the TS and the van der Waals structure bear a remarkable similarity, only a shortening and a slight bending of the intermolecular bond are required to attain the saddle-point configuration from the geometry of the complex. Thus, the orientations conducive to the formation of the HO–HCl complex are also favorable for the reaction and this complex is likely to act as a precursor for the reaction. On the basis of the theoretical calculations presented above, the negative steric asymmetry could be in-

terpreted as a manifestation of the van der Waals forces. Thus the experimental fact suggests that the HO–HCl well seems to influence the dynamics at this low collision energy. In the single-collision regime, if “formed,” the van der Waals complex is born with an excess of internal energy that may be used to surmount the reaction barrier and/or to (pre)dissociate the complex.

Besides the relative orientation of the reagents, the reactivity is also controlled by the height of the barrier to the reaction. This was estimated from the kinetic data to lie between 200 and 800 cm^{-1} and by theoretical calculations to be around 800–900 cm^{-1} .^{33,37–40} Yu and Nyman³³ found a vibrational adiabatic ground-state barrier height (V_a^G) of 810 cm^{-1} , but had to lower it to 350 cm^{-1} in order to obtain agreement with the experimental rate constants. Steckler *et al.*,³⁸ who calculated a higher barrier ($V_a^G=920 \text{ cm}^{-1}$) using the CCSD(T) method, appreciated an uncertainty much larger than 100 cm^{-1} due to the use of different basis sets for the calculation of the zero-point energies. Consequently, it is reasonable to assume that the real barrier to the reaction would be in the range of 300–800 cm^{-1} and that the collision energy of the present experiment (920 cm^{-1} with a FWHM of 250 cm^{-1}) is very likely to exceed the barrier. The reaction cross section at this collision energy was estimated to be 1.5 Å²,³³ quite similar in magnitude with the inelastic cross sections.³⁴ Moreover, Yu and Nyman³³ found that at low collision energies, the reaction between OH and HCl is dominated by the van der Waals forces determining tunneling effects. Supposing that the effect of the reactions is non-negligible, the OH molecules with favorable orientations may be removed from the detection region due to reactions. Under this hypothesis, the negative value obtained for the steric asymmetry factor can be interpreted not only as a reflection of the head-tail asymmetry of the PES, but also as an indication of possible reactions interfering in the dynamics at this collision energy.

The idea that the van der Waals well may influence the dynamics at low collision energies has some precedent, confirmed both experimentally and theoretically for the Cl+HD reaction. In this case, the weak van der Waals well, located in the entrance channel, has a substantial effect on the reaction branching ratio at low collision energies when HD is rotationally unexcited.⁴¹ Furthermore, recent five-dimensional (5D) quantum wave-packet calculations and a quasiclassical trajectory (QCT) study of the reaction probabilities for the OH+CO system indicate that the van der Waals interaction in the entrance channel is largely responsible for the reactivity at collision energies below 1650 cm^{-1} .^{42,43} The PES for the OH+CO system contains two linear van der Waals complexes, OH–CO ($D_e=700\text{--}800 \text{ cm}^{-1}$) and OH–OC ($D_e=400\text{--}500 \text{ cm}^{-1}$), and two reactive intermediates, *trans*-HOCO and *cis*-HOCO, with deep wells of about 10 000 cm^{-1} , which play an important precursor role connecting the reactants to the products.^{44–46} From electronic structure calculations it was found that the van der Waals complexes evolve directly into *cis/trans*-HOCO intermediates by intermolecular bending motion.⁴⁴ Due to the low reaction barrier ($V_a^G=400 \text{ cm}^{-1}$),⁴⁶ at the collision energy of 985 cm^{-1} , the molecules could

sample the whole PES. Taking into account these theoretical predictions, one may expect that the most favorable orientation for reactions occurs when the OH radicals are oriented with the H side towards CO, resulting in a positive steric asymmetry factor in agreement with the sign of the value measured for the scattering into the $\Omega=3/2, J=5/2, f$ state. The scattering of OH by N₂ exhibits a similar stereodynamics as the OH+CO system for rotational excitation into this state. According to Ref. 47, the deepest van der Waals well corresponds to a linear molecular structure with a binding energy (D_e) of about 460 cm^{-1} and is also located at the H side. From the comparison of the steric factors measured for low rotational excitation ($\Omega=3/2, J=5/2, f$) of OH as a result of collisions with HCl, CO, and N₂, one finds that the corresponding sign of the steric asymmetry factor is related to the orientation of the OH within the van der Waals complexes.

In contrast, the steric factor for the scattering of OH by HCl into the $\Omega=3/2, J=5/2, e$ state is very small and positive. A similar value was also measured for the collisions implying excitation into the $\Omega=3/2, J=7/2, e$ state. In turn, a large positive steric factor was measured for excitation into the $\Omega=3/2, J=9/2, e$ state, which seems to be at variance with the other values. We have shown above that the dynamics at these collision energies seems to be influenced by the van der Waals well, therefore we could also expect the formation of energized van der Waals complexes which would dissociate, releasing OH radicals with a preferential electronic orbital configuration. Unequal populations of the two Λ -doublet states corresponding to the two possible configurations of the OH electronic orbital were already found in the dissociation of water and of other OH-containing complexes.^{48,49}

The excitation into low rotational states of the $\Omega=1/2$ ladder is mainly governed by the difference potential V_{diff} , which according to recent *ab initio* calculations seems considerably less anisotropic than V_{sum} , and exhibits only a shallow well.³⁶ The experimental results are in agreement with this smaller anisotropy, resulting in a reduced influence of the OH orientation on the magnitude of the inelastic cross sections. We should note though that the steric factor for excitation into the $\Omega=1/2, J=5/2, f$ state is sensibly different from zero. The negative value of S could be due to the contribution to the scattering amplitude of the more anisotropic terms of the V_{sum} . This interference of V_{sum} in the scattering dynamics involving the spin-orbit-changing transitions is increasing with the excitation into higher rotational states for which the OH angular momentum coupling is no longer described by a pure Hund's case (a).⁵⁰

At the low collision energies used in the experiments investigating the scattering of OH by HCl, CO, and N₂, the long-range dipole-dipole and dipole-quadrupole interactions appear to dominate the dynamics at least for the lowest rotational excitation. However, it is also known that strong long-range anisotropic forces may induce a loss of the initial state orientation of the reactants, through trapping and reorientation effects.^{51,52} Trapping may cause a reduction of the steric effect for collisions taking place at large intermolecular distances. In this case, the collision partner being captured by

the partly attractive potential will fly around the target molecule and will collide with it on the side or even at the back. The reorientation effects consist of a change of the molecular axis orientation due to the same long-range forces, resulting in a reduction of the steric effect and may also be present over a wider range of impact parameters than trapping. In general, the collisions at large impact parameters are responsible for the excitation into low rotational states. Conversely, the collisions resulting in a large change in the internal energy will occur mostly at a small impact parameter. Consequently, the reduction of the steric effect may affect all final rotational states excited in the present experiment.

An inspection of the steric asymmetry factor S , measured for the highest rotational state excited in the present experiments, $\Omega=3/2$, $J=9/2$, f , reveals a reduction of its absolute value as compared with the values determined for excitation into lower- J states. If reorientation effects would take place, the prepared orientation would be scrambled as the molecular axis of the two partners would be steered by the long-range interaction into a preferred orientation. In these conditions, the scattering signals measured for the two initially prepared orientations will differ less and S will diminish and approach zero, which may explain the reduction of the steric factor for the transition to the $\Omega=3/2$, $J=9/2$, f state. Because OH is not rotating and has a lower inertia momentum than HCl due to the larger rotational constant, its axis would reorient easier. Besides, for HCl molecules which are rotating, the intermolecular axis cannot orient itself so easily. The strong dipole-dipole interactions may reorient some of the molecules initially oriented with the H side towards HCl in such a way that their O side would be more exposed to the HCl attack. The strength of the long-range interactions and the initial state of the colliding partner determine the degree of reorientation. As the long-range forces are the strongest for the interaction between OH and HCl, we also should expect stronger reorientation effects than in the case of OH+CO and OH+N₂ systems. In addition, assuming that the beam temperature is the same for all OH collision partners, about 20 K, the rotational population distribution will peak at higher rotational states for CO and N₂ as compared to HCl, for which the most populated states at this temperature are $J=0$ and $J=1$. For the former two, the long-range electrostatic forces are averaged over the rotational distribution, which will result in their further reduction as compared with those describing OH-HCl interaction and weaker reorientation effects are to be expected. Of course, the magnitude of the reorientation effects depends also on the time needed for the OH molecular axis to reorient itself as compared to the relative velocity. It is difficult to assess the reorientation issue for the excitation into the $\Omega=3/2$, $J=9/2$, f state, partially due to the large experimental uncertainties affecting the measurement of the corresponding steric factor. Therefore, additional experiments and theoretical calculations are required to provide higher accuracy information and a systematic survey of S by varying the initial conditions as relative velocity and rotational temperature.

V. SUMMARY

We address in this paper the stereodynamical issues occurring in the inelastic scattering of OH ($X^2\Pi$) radicals by HCl ($X^1\Sigma^+$). The experiments were performed in a crossed molecular-beam machine at the nominal collision energy of 920 cm⁻¹. The OH molecules were state selected in the lowest rotational state, $v=0$, $\Omega=3/2$, $J=3/2$, $M_J=3/2$, f , using a hexapole and subsequently oriented in a homogeneous electrical field. We have measured rotationally resolved relative cross sections for collisions in which OH is oriented with either the O side or the H side towards HCl, from which we have calculated the steric asymmetry factor S . The results are presented in comparison with data previously obtained by our group for the collisions of OH with CO ($E_{\text{coll}}=985$ cm⁻¹) and N₂ ($E_{\text{coll}}=985$ cm⁻¹) under similar experimental conditions. Once again, the comparison with these two systems points towards the fact that the PES is less head-tail symmetric with respect to the OH orientation for the interaction with HCl than for that with CO and N₂ as it was also indicated by the lack of Λ -doublet propensity found for the relative cross sections measured for collisions between HCl and nonoriented OH radicals.

A remarkable difference was observed for the scattering into low- J states where a preference for collisions at the H side (negative S) was found, while for the OH+CO/N₂ system the collisions at the O side (positive S) were preferred. A decrease in the negativity of the steric asymmetry factor seems to be apparent for the scattering into the highest J state, $\Omega=3/2$, $J=9/2$, f , as also found for the OH+N₂ system. For the interpretation of these results we have taken into account the anisotropy and the topology of the interaction potential governing both inelastic and reactive collisions. The presence of a well corresponding to the van der Waals complex located at the O side of OH and correlating with the transition state seems to play a role in the dynamics at this low collision energy. Moreover, from previous experimental and theoretical data we estimate that the collision energy of the present study should exceed the reaction barrier. The interference of reactions could also be used to explain the negative steric asymmetry factor obtained for the excitation into the $\Omega=3/2$, $J=5/2$, f state, as opposed to the positive value obtained for collisions of OH with CO for which the collisions at the H side would lead to reactions via the OH-CO van der Waals complex correlating with the HOCO intermediate. The decrease in the negativity of the steric asymmetry factor for higher rotational excitation may indicate that reorientation effects may influence the dynamics at this collision energy.

To summarize, the interpretation of our data in terms of the anisotropy of the PES indicates that the scattering dynamics at this collision energy (920 cm⁻¹) may be influenced by the HO-HCl van der Waals well and by the reorientation effects determined by the long-range electrostatic forces and may as well involve reactive collisions. Additional experiments of the OH+HCl system concerning studies of reactive collisions and van der Waals complexes would be very useful in ascertaining the proposed explanations and understanding

its dynamics. A reactive study at this low collision energy may seem very challenging, as the reactive cross sections are predicted to be quite small, but we expect it to be feasible by the application of the sensitive REMPI technique for the detection of the atomic reaction product. Furthermore, by extending the investigation of the system dynamics over a wider energy regime, one can establish the influence of the reorientation effects and the relative contribution of the reactive channel. Another way of verifying the interpretation proposed herein would be to perform similar inelastic-scattering measurements involving the isotopomers of OH and/or HCl that will sample different regions of the respective potential-energy surfaces (PESs) involving higher reaction barriers due to the change in the zero-point energy (ZPE) and possibly slightly more bound van der Waals complexes. An important step in understanding the stereodynamics of this system at low collision energies can be made with the help of quasiclassical trajectories and quantum scattering calculations. For a meaningful comparison with experimental results, it is necessary to obtain inelastic and reactive cross sections using potential-energy surfaces, which include accurate descriptions of the van der Waals and transition state regions.

ACKNOWLEDGMENTS

The authors wish to thank Leander Gerritsen and Peter Claus for their expert technical assistance, Professor A. van der Avoird, Dr. G. Groenenboom, and Dr. J. Klos for stimulating discussions, and Dr. M. Brouard for a critical reading of the manuscript. Financial support from the European Commission through the RTN program (RTN Reaction Dynamics), Contract No. HPRN-CT-1999-0007, is gratefully acknowledged.

- ¹R. D. Levine and R. B. Bernstein, *Molecular Reaction Dynamics and Chemical Reactivity* (Oxford University Press, New York, 1987).
- ²D. P. Pullmann, B. Friedrich, and D. R. Herschbach, *J. Chem. Phys.* **93**, 3224 (1990).
- ³V. Aquilanti, D. Ascenzi, D. Cappelletti, and F. Pirani, *Nature (London)* **371**, 399 (1994).
- ⁴F. Pirani, D. Cappelletti, M. Bartolomei, V. Aquilanti, M. Scotoni, M. Vescovici, D. Ascenzi, and D. Bassi, *Phys. Rev. Lett.* **86**, 5035 (2001).
- ⁵R. C. Estler and R. N. Zare, *J. Am. Chem. Soc.* **100**, 1323 (1978).
- ⁶M. J. Weida and C. S. Parmenter, *J. Chem. Phys.* **107**, 7138 (1997).
- ⁷M. S. de Vries, V. I. Srdanov, C. P. Hanrahan, and R. M. Martin, *J. Chem. Phys.* **78**, 5582 (1983).
- ⁸H. Stapelfeldt and T. Seideman, *Rev. Mod. Phys.* **75**, 543 (2003), and references therein.
- ⁹H. J. Loesch and J. Remscheid, *J. Chem. Phys.* **93**, 4779 (1990).
- ¹⁰B. Friedrich and D. R. Herschbach, *Z. Phys. D: At., Mol. Clusters* **18**, 153 (1991).
- ¹¹M. Wu, R. J. Bemish, and R. E. Miller, *J. Chem. Phys.* **101**, 9447 (1994).
- ¹²P. R. Brooks, J. S. McKillop, and H. G. Pippin, *Chem. Phys. Lett.* **66**, 144 (1979).
- ¹³S. Stolte, in *Atomic and Molecular Beam Methods*, edited by G. Scoles (Oxford University Press, New York, 1988), p. 631.
- ¹⁴D. H. Parker and R. B. Bernstein, *Annu. Rev. Phys. Chem.* **40**, 561

- (1989).
- ¹⁵B. Friedrich and D. R. Herschbach, *J. Phys. Chem. A* **103**, 10280 (1999).
- ¹⁶H. Sakai, S. Minemoto, H. Nanjo, H. Tanji, and T. Suzuki, *Phys. Rev. Lett.* **90**, 083001 (2003).
- ¹⁷R. D. Levine, *Chem. Phys. Lett.* **175**, 331 (1990).
- ¹⁸I. W. M. Smith, *J. Chem. Educ.* **59**, 9 (1982).
- ¹⁹E. Pollack and R. E. Wyatt, *J. Chem. Phys.* **78**, 4464 (1983).
- ²⁰R. D. Levine and R. B. Bernstein, *Chem. Phys. Lett.* **105**, 467 (1984).
- ²¹I. Schechter and R. D. Levine, *J. Chem. Soc., Faraday Trans. 2* **85**, 1059 (1989).
- ²²R. B. Bernstein, D. R. Herschbach, and R. D. Levine, *J. Phys. Chem.* **91**, 5365 (1987).
- ²³A. J. Orr-Ewing, *J. Chem. Soc., Faraday Trans.* **92**, 881 (1996).
- ²⁴J. J. van Leuken, J. Bulthuis, S. Stolte, and J. G. Snijders, *Chem. Phys. Lett.* **260**, 595 (1996).
- ²⁵M. H. Alexander and S. Stolte, *J. Chem. Phys.* **112**, 8017 (2000).
- ²⁶A. Gijsbertsen, M. J. L. de Lange, A. E. Wiskerke, H. Linnartz, M. Drabbels, J. Klos, and S. Stolte, *Chem. Phys.* **301**, 293 (2004).
- ²⁷M. J. L. de Lange, S. Stolte, C. A. Taatjes, J. Klos, G. C. Groenenboom, and A. van der Avoird, *J. Chem. Phys.* **121**, 11691 (2004).
- ²⁸K. Schreel and J. J. ter Meulen, *J. Phys. Chem. A* **101**, 7639 (1997).
- ²⁹M. C. van Beek and J. J. ter Meulen, *J. Chem. Phys.* **115**, 1843 (2001).
- ³⁰M. C. van Beek, J. J. ter Meulen, and M. H. Alexander, *J. Chem. Phys.* **113**, 637 (2000).
- ³¹J. Schleipen and J. J. ter Meulen, *Chem. Phys.* **156**, 479 (1991).
- ³²R. Cireasa, M. C. van Beek, A. Moise, and J. J. ter Meulen, *J. Chem. Phys.* **122**, 074319 (2005).
- ³³H.-G. Yu and G. Nyman, *J. Chem. Phys.* **113**, 8936 (2000).
- ³⁴G. Lendvay, *Abstr. Pap. - Am. Chem. Soc.* **218**, 202 (1999).
- ³⁵J. Klos, J. Aoiz, R. Cireasa, and J. J. ter Meulen, *Phys. Chem. Chem. Phys.* **6**, 4968 (2004).
- ³⁶J. Klos, G. Dhont, P. Wormer, and A. van der Avoird (private communication) (unpublished).
- ³⁷A. Rodriguez, E. Garcia, M. L. Hernandez, and A. Laganà, *Chem. Phys. Lett.* **371**, 223 (2003).
- ³⁸R. Steckler, G. M. Thurman, J. D. Watts, and R. J. Bartlett, *J. Chem. Phys.* **106**, 3926 (1997).
- ³⁹N. I. Butkovskaya and D. W. Setser, *J. Chem. Phys.* **108**, 2434 (1998).
- ⁴⁰IUPAC database (Subcommittee for Gas Kinetics Data Evaluation), <http://www.iupac-kinetic.ch.cam.ac.uk>
- ⁴¹D. Skouteris, D. E. Manolopoulos, W. Bian, H.-J. Werner, L.-H. Lai, and K. Liu, *Science* **26**, 1713 (1999).
- ⁴²M. J. Lakin, D. Troya, G. C. Schatz, and L. B. Harding, *J. Chem. Phys.* **119**, 5848 (2003).
- ⁴³R. Valero, D. A. McCormack, and G.-J. Kroes, *J. Chem. Phys.* **120**, 4263 (2004).
- ⁴⁴M. I. Lester, B. V. Pond, D. T. Anderson, L. B. Harding, and A. F. Wagner, *J. Chem. Phys.* **113**, 9889 (2000); M. I. Lester, B. V. Pond, M. D. Marshall, D. T. Anderson, L. B. Harding, and A. F. Wagner, *Faraday Discuss. Chem. Soc.* **118** (2001).
- ⁴⁵K. Kudla, A. G. Koures, L. B. Harding, and G. C. Schatz, *J. Chem. Phys.* **96**, 7465 (1992).
- ⁴⁶H.-G. Yu, J. T. Muckerman, and T. J. Sears, *Chem. Phys. Lett.* **349**, 547 (2001), and references therein.
- ⁴⁷M. I. Lester, R. A. Loomis, R. L. Schwartz, and S. P. Walch, *J. Phys. Chem. A* **101**, 9195 (1997); M. D. Marshall, B. V. Pond, S. M. Hopman, and M. I. Lester, *J. Chem. Phys.* **114**, 7001 (2001).
- ⁴⁸P. Andresen, G. S. Ondrey, B. Titze, and E. W. Rothe, *J. Chem. Phys.* **80**, 2548 (1984).
- ⁴⁹B. V. Pond and M. I. Lester, *J. Chem. Phys.* **118**, 2223 (2003).
- ⁵⁰P. J. Dagdigian, M. H. Alexander, and K. Liu, *J. Chem. Phys.* **91**, 839 (1989).
- ⁵¹R. B. Bernstein and R. D. Levine, *J. Phys. Chem.* **93**, 1687 (1989).
- ⁵²G. C. Groenenboom and A. J. H. M. Meijer, *J. Chem. Phys.* **101**, 7592 (1994).